EV Charging Station Integrating Renewable Energy and Second–Life Battery

Ahmad Hamidi, Luke Weber, and Adel Nasiri

Department of Electrical and Computer Engineering
University of Wisconsin–Milwaukee
Milwaukee, USA
Email: nasiri@uwm.edu; URL: www.uwm.edu/~nasiri

Abstract—**This paper investigates the integration of wind power, Photovoltaic (PV) solar power, and Li–Ion battery energy storage into a DC microgrid–based charging station for Electric Vehicles (EVs). The goal is for the Renewable Energy (RE) sources to provide as much of the charging energy as possible. The facility will be grid connected so that charging can occur during cloudy, windless days. The grid connection also permits exporting power when generation exceeds demand within the microgrid. It is proposed that second–life lithium–ion batteries be integrated into the proposed system to serve as an energy buffer and provide emergency energy upon loss of the grid connection. The Simulink modeling and simulation components of the charging station includes the solar PV, wind, EV batteries, and second–life batteries with their associated controls. The battery model is based on laboratory tests conducted during the project. Control functions and algorithms enabling the system to operate in various modes are developed, and simulation results are presented.**

Keywords– Energy Storage System; Renewable Energy; Second–Life Battery.

I. INTRODUCTION

An increasing saturation of EVs will require a proliferation of charging stations, perhaps at corporate sites or car parks with connections to public transport. For various reasons – including environmental concerns and energy costs – it is preferable to use Renewable Energy (RE) sources to charge EVs. This paper proposes a low cost energy storage solution which integrates second–life EV batteries to buffer the intermittent nature of resources like wind and solar. As intermittent resources comprise an increasing percentage of system generation capacity compared to traditional hydraulic and thermal synchronous generation, new challenges to the integrity, stability, and reliability of the utility grid arise. Combining energy storage with renewable sources can reduce the adverse impacts on utility grids by reducing intermittency. Hybrid and plug–in hybrid electric technologies are playing a role in increasing fuel efficiency and reducing emissions of new EVs. Energy storage systems are an integral part of these technologies. Lithium–ion batteries are one the most desirable energy storage types due to their relatively long lifetime, fast response, high energy and power densities, and decreasing costs. These characteristics make this type of batteries a cost effective candidate for renewable energy integration and automotive applications.

The proposed system in this paper is an integration of wind power, Photovoltaic (PV) solar power, and Li–Ion battery energy storage into a DC microgrid–based charging station for EVs. The charging stations are appropriate for corporate sites or car parks with connections to public transport. EVs will be parked at the facility when combined PV and wind sources will generally be able to deliver energy. System architecture is presented in the Section II. Electric battery, wind and solar PV models are presented in Section III. The EV charging station layout is presented in Section IV. Simulation results of the EV charging station are discussed in Section V. Section VI lists the conclusions.

II. SYSTEM ARCHITECTURE

The proposed system topology of a DC microgrid is presented in Fig. 1. A wind turbine and a PV solar array integrated with batteries provide energy for the EV charging station. The station is grid connected to permit the export or import of energy as instructed by the control system. The main goal is supplying the EV charging facility, storing surplus energy by charging the second–life batteries. The control objective is to capture the maximum available energy from the sunlight and wind while maintaining power output to the grid as stable as possible. The second–life batteries will be charged or discharged to: buffer the generated power delivered to the EV batteries and grid, and send energy to charge the EV batteries in cases of renewable source shortages.
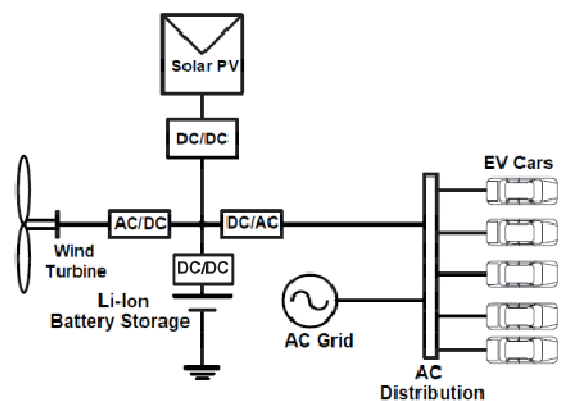

Figure 1. Block diagram of the EV Charging Station with Renewable Energy Sources.

III. MODELING OF RENEWABLE ENERGY SOURCES AND BATTERY ENERGY STORAGE SYSTEM

A. Wind Power Modeling

Simulink models for the wind power system include the wind turbine, wind generator and AC/DC converter components. The wind turbine is modeled from an electromechanical point of view. The model provides a representation of the aerodynamic behavior of the rotor including the pitch control system and the maximum power point characteristic [1]. This kind of wind turbine is characterized by the absence of a gearbox and the presence of a back–to– back converter sized for the whole power, as shown in Fig. 2. The wind turbine model is mechanically coupled to a 550kW Permanent Magnet Synchronous Generator (PMSG). The PMSG connects to the DC link via an AC/DC converter. A current vector technique is utilized to control the active and reactive output power of the PMSG.
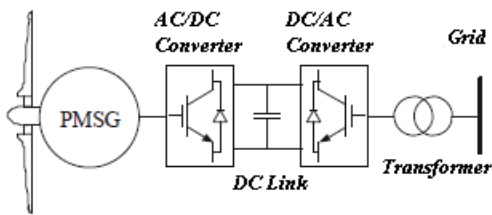

Figure 2.   Schematic diagram of a wind power system connected to grid.

The operating regions of a wind turbine can be illustrated by its power curve, which gives the estimated power output as a function of wind speed. Three distinct wind speed regions are typical of wind turbine power curves. A control method for turbine pitch has been applied for the third region, where the wind speed is above nominal wind speed. Once the wind speed exceeds the rated speed value, the pitch angle control system has to reduce the aerodynamic efficiency by increasing the blade attack angle. The control is sensitive to rotational speed: if speed goes above 1 per unit, the PI control system commands a blade pitch angle increase.

In the second region – where turbine power output is proportional to the cube of wind speed – maximum turbine efficiency is achieved when the tip speed ratio is held within a narrow band. The Maximum Power Point Tracking (MPPT) algorithm has to control the generator rotational speed to achieve the desired power output. This tracking action is realized by tracking the curve, shown in Fig. 3, which generates the reference active power as a function of the rotational speed of the turbine.

The wind converter is an AC to DC rectifier implemented with IGBT switches. Vector control techniques are used to maintain wind power system output at the highest output. Based on the rotor speed, reference power from the MPPT lookup table is applied to the power regulator block, while the reactive power reference is held to zero. The power regulator produces reference current in the dq rotating frame [2].
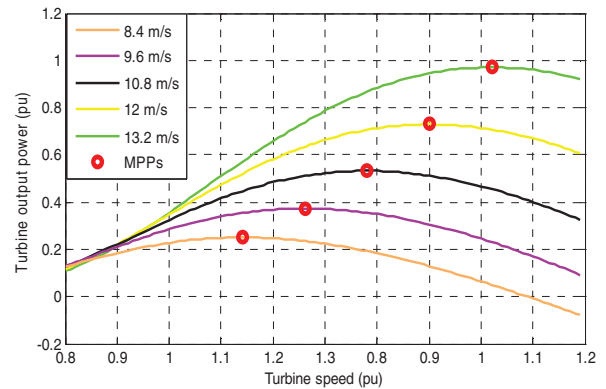

Figure 3.   Turbine Characteristics and the Maximum Power points (MPPs)

B. PV Solar Power Modeling

An electrical model capable of emulating the Current vs. Voltage (I–V) and Power vs. Voltage (P–V) behavior of the PV cell under different irradiances [3] has been implemented in the Matlab/Simulink environment. In this model, temperature is considered constant at standard ambient temperature in order to minimize the execution time of the overall model. (It is recognized that temperature has a significant effect on the I–V and P–V output characteristic curves of the cell, but analysis of the potential impact is out of scope for this project.) The model enables simulating different array topologies by altering the series/parallel PV cell connections PV.

A PV array with 264 parallel strings of 7 modules in series is modeled. The array is rated to generate about 560 kW power under full sun conditions. Fig. 4 shows typical I–V and P–V characteristics of a photovoltaic module. A MPPT algorithm is applied to ensure the PV array is operating at maximum power output based on irradiance (under the assumption of constant operating temperature). A Perturbation and Observation (P&O) method – where the output voltage is altered frequently to detect the optimal array voltage – has been employed in this research work. This is a common MPPT algorithm applied in many PV systems, is simple to implement, and works well when the irradiation does not change quickly over time [4].
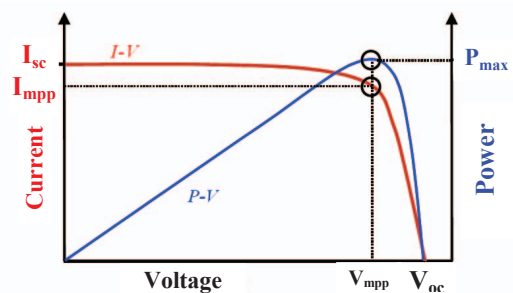

Figure 4.   P–V and I–V characteristic of a typical PV cell.

A DC to DC boost converter is utilized to transfer power from the PV array to the DC bus – Fig. 5. The converter output is set to match the DC bus voltage amplitude, while the input tracks the voltage that generates maximum power. Implementation of the P&O MPPT algorithm takes the form of Matlab code written to generate gate pulses for the converter switches.
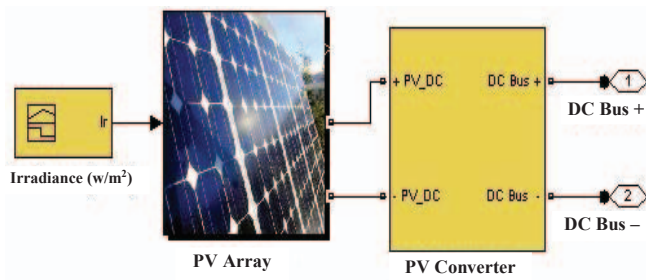
Figure 5.   Solar PV array and PV converter.

C. Battery Energy Storage System (BESS) Modeling

1) Proposed Electrical Battery Model

According to literature published in the last decade, battery models can be categorized into three groups: electrochemical, mathematical and electrical. Of these three, only the electrical model has the ability to represent the I–V characteristics of the battery.

Electrical battery models also divide in three categories: Thevenin, Impedance and Runtime based [5]. Table 1 presents a brief comparison of advantages and disadvantages of each model.

TABLE I.   COMPARISON OF ELECTRICAL MODELS [5].

Predicting Capability	Thevenin–Based	Impedance–Based	Runtime–Based
DC	No	No	Yes
AC	Limited	Yes	No
Transient	Yes	Limited	Limited
Battery Runtime	No	No	Yes

For a comprehensive and accurate representation, a model which combines the transient capability of Thevenin–based, the AC features of Impedance–based, and the runtime information of the Runtime–based model is proposed. The model is based on the electrical battery model presented in [5], with a third RC network added to emulate very small time constants to represent the transient battery response. Fig.6 illustrates the proposed battery model.
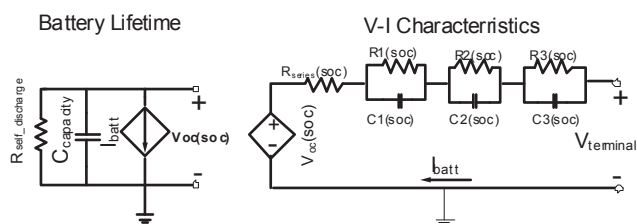

Figure 6.   The proposed electrical battery model.

The model consists of two parts: battery lifetime on the left hand side of the Fig. 6 – to embody the capacity and state of charge, and capture runtime information; and the V–I characteristics on the right – to represent the transient battery response.

The battery lifetime has been modeled using three elements: a resistance $R_{self\_discharge}$ characterizes self discharge energy loss, a capacitance $C_{capacity}$ provides the state of charge of the battery as a scaled voltage drop, and a current–dependent current source I_{batt} accounts for charging and discharging $C_{capacity}$. $C_{capacity}$ represents the charge stored in the battery by

converting nominal battery capacity in Ah to charge in coulombs, and its value is defined in [5,6]:

$$C_{Capacity} = 3600 \cdot Capacity \cdot f_1(cycle) \cdot f_2(temp) \\ f_3(current\ rate) \qquad (1)$$

Where Capacity is the nominal battery capacity in Ah and f_1 (cycle), f_2 (temp) and f_3 (current rate) are cycle number, temperature and current rate dependent correction factors, respectively.

The V–I representation on the right hand side of the Fig. 6 is used to model the transient response of the battery. All elements on the right side are multivariable functions of the SOC, current, temperature, and number of charge and discharge cycles. For this analysis, the elements are simulated as functions of the SOC and battery lifetime only [6]. To model the nonlinear relationship between open–circuit voltage and the SOC, a voltage dependent voltage source $V_{oc(SOC)}$ is used. The resistor R_{series} is responsible for immediate voltage drop in the step response.

Three RC networks are utilized to represent the multiple time constant transient response of the battery. There is a tradeoff between calculation cost and accuracy of the transient response: by increasing the number of RC transient circuits, the execution time, memory required and accuracy will be increased while the modeling error will be decreased [7,8].

2) Test Procedure, Model Extraction and Verification

To extract all the parameters introduced by the proposed model a test bed and test procedure were developed. The system includes a DC digitally programmable load, a DC source, a current sensor, National Instruments CompactRIO and LabVIEW software – see Fig. 7. The DC load and source were connected to the CompactRIO serial port for communication with the LabVIEW interface.   A breaker contactor provides disconnection for the DC source during discharging periods. A CompactRIO analog IO differential module digitizes and carries the measured current and voltage signals at each sampling instance to the LabVIEW interface. A model was developed in the LabVIEW environment for collecting data, and performing charge and discharge cycling.
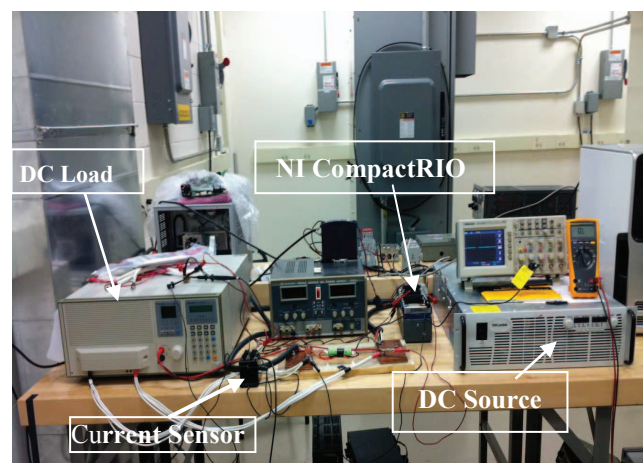

Figure 7.   Test bed for the battery.

To identify the electrical model parameters, several tests were designed and conducted on two each new and second–life 2.6 Ah cylindrical Li–ion batteries. The tests include pulsed and constant current charging and discharging at different capacity rates – 0.2C, 0.5C, 1C and 2C. Components of the

model have been derived from detailed analyses of dynamic and steady state testing. Further details on model extraction are found in [9,10]. The model is implemented in Matlab/Simulink and verified by comparing the simulation results to experimental data – see Fig. 8.
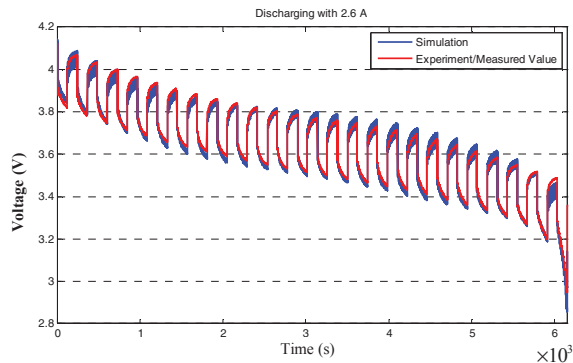

Figure 8. Terminal voltage of the battery Simulink model and experimental data.

Based on the proposed model for the second–life battery, a pack of batteries has been simulated to provide 160 Ah, 160kW. The battery pack is connected to the DC link via a bi–directional buck/boost converter. The converter boosts the battery pack terminal voltage to the DC bus voltage magnitude. A controller has been designed to determine the battery charge and discharge cycles based on load demand and generated energy, as shown in Fig. 9.
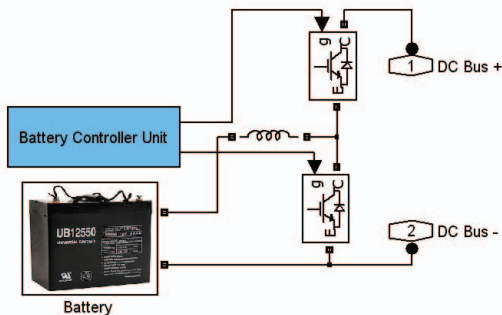

Figure 9. Battery converter and controller unit.

IV. CHARGING STATION LAYOUT

An overview of the layout of the EV facility is depicted in Fig. 10. The wind turbine and a PV solar array are integrated with a pack of life batteries.

For the grid side inverter control, a vector control scheme has been implemented that regulates the DC bus voltage and controls the power flow between the DC bus and the AC grid. The scheme is based on a synchronously rotating stator flux oriented d–q reference frame, aligning the d–axis component with grid d–axis voltage vector, and setting the q component to zero [2].
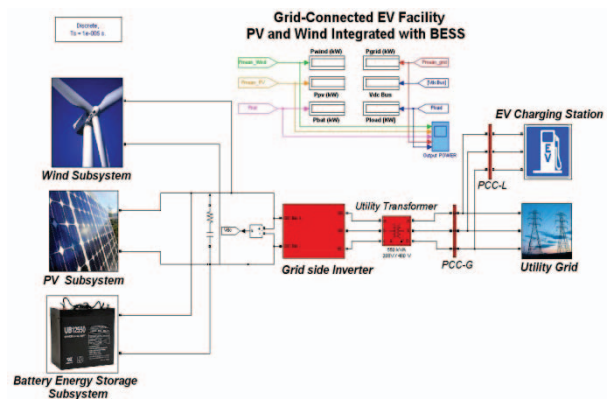

Figure 10. The layout of the EV charging facility modeled in Matlab/Simulink.

V. SIMULATION AND RESULTS

Simulations are performed to show the behavior of each subsystem. The dynamic response of the wind turbine, wind generator, PV subsystem and storage subsystem are tested. Detailed modeling is performed on the component and system levels, and the results are presented in Fig. 11.

The wind speed profile for v_{wind} has two constituent parts expressed as:

$$v_{wind}(t) = v_{wind\_mean} + v(t) \qquad (2)$$

where $v_{wind-mean}$ is the mean wind speed and $v(t)$ is the instantaneous turbulent component – a random signal with zero mean and variance of 5.

To evaluate the interaction between the subsystems, load, and grid in the proposed system, a specific irradiance profile has been applied to the PV solar array to simulate full sun irradiance and sun irradiance lower than 200 W/m^2 as shown in Fig. 11.
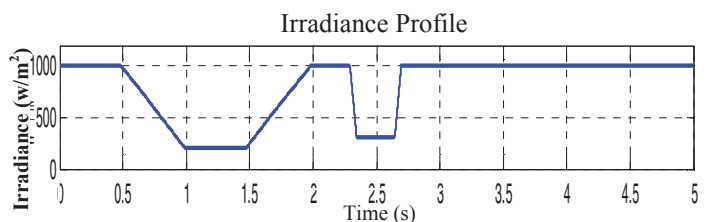

Figure 11. Irradiance profile injected to the PV array model.

For the test case shown in Fig. 12 – excepting the initial transient – the PV operates at its nominal output power during the initial 0.5 seconds as shown in Fig. 12.b. During that time period, wind power is increasing in magnitude as shown in Fig. 12.a. Since the combined energy generated is greater than the demand – Fig. 13.b. – part of the surplus is sent to the battery for storage as indicated in Fig. 12.c, and the balance is injected into the grid as seen in Fig. 13.a.

From 0.5 thru 1 second, wind power is still increasing but PV output has a negative slope due to the irradiance profile. Consequently, the total generated power falls below the demand level near 0.6 seconds, the battery starts discharging,

and no power is exchanged with the grid between ~0.6 to 1.0 seconds.

The generation shortfall between 1 and 1.5 seconds is less than the battery rating of 160kW so the battery is not being discharged at its full power rating. At 1.5 second, wind power reaches a steady state value and remains there for the rest of the simulation. However, PV power passes another up and down cycle and then maintains full rated power output starting at ~2.75 seconds. DC bus voltage is kept constant at 700V during the simulation as shown in Fig. 13.c.
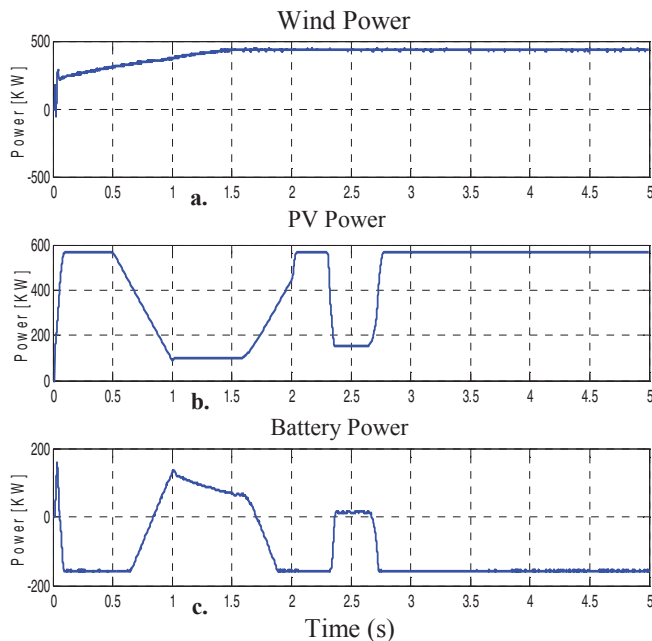

Figure 12. The station power flow.

Figure 13. Grid power flow, load power and DC bus voltage.

VI. CONCLUSION

A DC–based microgrid EV charging station using second–life Li–Ion batteries as bulk storage, and wind and solar PV energy sources has been presented. Detailed models for the wind turbine and solar PV have been developed, including practical constraints and MPPT control algorithms. Comprehensive models for second–life EV batteries have been developed from test results. Control logic has been employed to absorb maximum power from the renewable sources and charge the EVs. Second–life batteries are utilized to buffer energy exchange with the utility grid.

VII. ACKNOWLEDGMENT

REFERENCES

[1] Ackermann, "Wind Power in Power Systems", John Wiley and Sons Ltd, ISBN: 0470855088, New York, 2005.

[2] R. Teodorescu, M. Liserre, P. Rodríguez, "Grid Converters for Photovoltaic and Wind Power Systems", John Wiley & Sons Ltd, ISBN 978–0–470–05751–3, 2011.

[3] Huan–Liang Tsai, Ci–Sang Tu, Yi–Jie Su, "Development of the generalized photovoltaic model using MATLAB/Simulink", in Proceedings of the World Congress on Engineering and Computer Science 2008 WCECS, October 22–24, 2008, San Francisco, USA.

[4] J. Hui, A. Bakhshai and P. K. Jain, "A Hybrid Wind–Solar Energy System: A New Rectifier Stage Topology", Applied Power Electronics Conference and Exposition (APEC), 2010.

[5] M. Chen, G. A. Rincon–Mora, "Accurate Electrical Battery Model Capable of Predicting Runtime and I–V Performance", *IEEE Transactions on Energy Conversion.*, vol. 21, no. 2, pp. 504–511, June 2006.

[6] R. C. Kroeze, P.T. Krein, "Electrical battery model for use in dynamic electric vehicle simulations," *IEEE Power Electronics Specialists Conference, PESC 2008.*

[7] B. Schweighofer, K. M. Raab, and G. Brasseur, "Modeling of high power automotive batteries by the use of an automated test system", IEEE Trans. Instrum. Meas., vol. 52, no. 4, pp. 1087–1091, Aug. 2003.

[8] H. Zhang and M.Y. Chow, "Comprehensive Dynamic Battery Modeling for PHEV Applications", Power and Energy Society General Meeting, IEEE, 2010.

[9] S. Abu–Sharkh, D. Doerffel, "Rapid test and non–linear model characterization of solid–state lithium–ion batteries", *Journal of Power Sources 130 (2004)*, pp. 266–274, Dec. 2003.

[10] L.Gao, S. Liu, "Dynamic Lithium–Ion Battery Model for System Simulation", *IEEE Transactions on Components and Packaging Technologies,* vol. 25, no. 3, pp. 495–505, Sept. 2002.